HHS Public Access

Author manuscript

Brain Struct Funct. Author manuscript; available in PMC 2018 May 07.

Published in final edited form as:

Brain Struct Funct. 2017 December ; 222(9): 4111–4129. doi:10.1007/s00429-017-1456-5.

Sexually dimorphic distribution of Prokr2 neurons revealed by the Prokr2-Cre mouse model

Zaid Mohsen[1], **Hosung Sim**[1], **David Garcia-Galiano**[1], **Xingfa Han**[1,2], **Nicole Bellefontaine**[1], **Thomas L. Saunders**[3,4], and **Carol F. Elias**[1,5]

[1]Department of Molecular and Integrative Physiology, University of Michigan, 1137 E. Catherine St., 7732B Med Sci II, Ann Arbor, MI 48109-5622, USA

[2]Isotope Research Lab, Sichuan Agricultural University, Ya'an 625014, People's Republic of China

[3]Department of Internal Medicine, University of Michigan, Ann Arbor, MI, USA

[4]University of Michigan Transgenic Animal Model Core, Ann Arbor, MI, USA

[5]Department of Obstetrics and Gynecology, University of Michigan, Ann Arbor, MI, USA

Abstract

Prokineticin receptor 2 (PROKR2) is predominantly expressed in the mammalian central nervous system. Loss-of-function mutations of *PROKR2* in humans are associated with Kallmann syndrome due to the disruption of gonadotropin releasing hormone neuronal migration and deficient olfactory bulb morphogenesis. PROKR2 has been also implicated in the neuroendocrine control of GnRH neurons post-migration and other physiological systems. However, the brain circuitry and mechanisms associated with these actions have been difficult to investigate mainly due to the widespread distribution of Prokr2-expressing cells, and the lack of animal models and molecular tools. Here, we describe the generation, validation and characterization of a new mouse model that expresses Cre recombinase driven by the *Prokr2* promoter, using CRISPR-Cas9 technology. Cre expression was visualized using reporter genes, tdTomato and GFP, in males and females. Expression of Cre-induced reporter genes was found in brain sites previously described to express Prokr2, e.g., the paraventricular and the suprachiasmatic nuclei, and the area postrema. The Prokr2-Cre mouse model was further validated by colocalization of Cre-induced GFP and Prokr2 mRNA. No disruption of *Prokr2* expression, GnRH neuronal migration or fertility was observed. Comparative analysis of Prokr2-Cre expression in male and female brains revealed a sexually dimorphic distribution confirmed by in situ hybridization. In females, higher Cre activity was found in the medial preoptic area, ventromedial nucleus of the hypothalamus, arcuate nucleus, medial amygdala and lateral parabrachial nucleus. In males, Cre was higher in the amygdalo-hippocampal area. The sexually dimorphic pattern of Prokr2 expression indicates differential roles in reproductive function and, potentially, in other physiological systems.

Keywords

Kallmann syndrome; Infertility; GnRH migration; HPG axis; CRISPR/Cas9

Correspondence to: Carol F. Elias.

Introduction

Prokineticin receptor 1 and 2 (PROKR1 and PROKR2) are G-protein coupled receptors (GPCR) for two secreted chemokines: the prokineticins 1 and 2 (PROK1 and PROK2) (Lin et al. 2002; Masuda et al. 2002; Soga et al. 2002). Whereas *Prokr1* is highly expressed in peripheral tissues, *Prokr2* is predominately expressed in the central nervous system (Soga et al. 2002). In the mouse brain, *Prokr2* is widespread in multiple nuclei from the olfactory bulb to the brainstem (Cheng et al. 2006). Mice with loss-of-function mutations in *Prok2* or *Prokr2* genes have undeveloped olfactory bulb and related tracts (Matsumoto et al. 2006; Ng et al. 2005; Prosser et al. 2007). These mice also show deficient gonadotropin-releasing hormone (GnRH) neuronal migration, atrophy of the reproductive organs and infertility (Matsumoto et al. 2006; Pitteloud et al. 2007). These findings made the PROK2/PROKR2 signaling deficient mice a relevant preclinical model of Kallmann syndrome, which is the combination of hypogonadotropic hypogonadism (HH) with reduced (hyposmia) or absent (anosmia) sense of smell due to impaired olfactory development (Abreu et al. 2010; Martin et al. 2011). In agreement with this observation, a subset of humans diagnosed with Kallmann syndrome shows loss-of-function mutations in *PROK2* or *PROKR2* genes (Cole et al. 2008; Dodé et al. 2006; Pitteloud et al. 2007).

Following these initial reports, a series of findings demonstrated that the Prok2/Prokr2 system is more complex than previously anticipated (Abreu et al. 2012; Balasubramanian et al. 2011). For example, whereas homozygous mutations in mice are necessary for the reproductive and olfactory deficits, in humans these effects are found in heterozygous mutations (Abreu et al. 2008; Canto et al. 2009; Cole et al. 2008; Leroy et al. 2008; Monnier et al. 2009; Sarfati et al. 2010; Sinisi et al. 2008). However, in the heterozygous state, a high degree of heterogeneity across families and within members of the same family has been reported (Cole et al. 2008; Dodé et al. 2006). Moreover, in about 30% of humans with mutations in the *PROK2* or *PROKR2* genes reproductive failure occurs with apparently normal olfactory bulb formation. Mice heterozygous for *Prok2* and/or *Prokr2* loss-of-function mutation(s) also show reproductive deficits in the face of normal olfactory bulb morphogenesis and GnRH neuronal migration (Xiao et al. 2014). These observations suggest the *Prok2/Prokr2* system has an intricate action in neurodevelopment and normal physiology in adulthood. They also demonstrate a neuroendocrine role for the *Prok2/Prokr2* independent of the effects in neuronal migration (Cole et al. 2008; Martin et al. 2011).

In addition to reproductive dysfunction, abnormal circadian rhythms in thermogenesis, physical activity, corticosterone secretion and glucose homeostasis have been documented in mice lacking *Prok2* and/or *Prokr2* expression (Cheng et al. 2002; Hu et al. 2007; Li et al. 2006; Prosser et al. 2007; Zhou and Cheng 2005). Despite the availability of mouse gene knockout models, the neural circuitry and molecular mechanisms associated with these physiological deficits have been difficult to determine. The widespread distribution of Prokr2 in the brain and the developmental arrest of mice with *Prokr2* loss-of-function mutation preclude the use of the global knockout model to assess adult physiology. To overcome these issues and increase the opportunities to investigate the *Prokr2* system, we developed a knock-in mouse line using the CRISPR-Cas9 technology in which Cre

recombinase is driven by the *Prokr2* promoter without disrupting the *Prokr2* gene. Here, we describe the generation, validation and the comparative distribution of Prokr2-Cre expression in male and female adult brain. We also assess the potential changes in *Prokr2* gene expression, GnRH neuronal migration and fertility in these mice to determine if the Cre transgene changed the *Prokr2* expression and function.

Materials and methods

Animals

Adult male and female B6;SJL-*Prokr2*$^{em1(cre)Cfe}$ (named Prokr2-Cre), B6.Cg-*Gt*(*ROSA*)*26Sor*$^{tm14(CAG-tdTomato)Hze}$/J (R26-tdTom) (JAX® mice, stock # 007914), B6;129-*Gt*(*ROSA*)*26Sor*^{tm2Sho}/J (R26-GFP) (JAX mice, stock # 004077) and C57BL/6J (JAX mice, stock # 00064) mice were maintained in the University of Michigan animal facility in a light- (12 h on/off) and temperature-controlled (21–23 °C) environment with free access to water and food. Mice were fed phytoestrogen-reduced Envigo diet 2016 (16% protein/4% fat), except during breeding when they were fed higher protein and fat phytoestrogen-reduced Envigo diet 2019 (19% protein/8% fat). A phytoestrogen reduced diet was used to avoid the effect of exogenous estrogen in reproductive physiology. All procedures and experiments were carried out in accordance with the guidelines established by the National Institutes of Health Guide for the Care and Use of Laboratory Animals and approved by the University of Michigan Institutional Animal Care and Use Committee (Animal Protocol No. 04380). The R26-tdTomato and R26-GFP mice carry targeted mutations of the *ROSA26* locus with a loxP-flanked transcriptional blocking cassette preventing the expression of CAG promoter-driven tdTomato or enhanced green fluorescent protein (GFP) reporters, respectively. Cre-mediated excision of the loxP-flanked transcription blocking cassette allows the expression of tdTomato or GFP. All mice were genotyped before and after experiments by extracting DNA from tail tip biopsies (RED Extract-N-Amp Tissue PCR Kit catalog no. XNAT, Sigma, St. Louis, MO, USA) and performing PCR. The genotyping primers are described in Table 1.

Generation of Prokr2-Cre mice using CRISPR/Cas9 technology

We used the Clustered Regularly Interspaced Short Palindromic Repeats associated protein Cas9 (CRISPR/Cas9) technology (Cong et al. 2013; Mali et al. 2013) to generate a transgenic mouse line that expresses Cre recombinase in Prokr2-expressing cells. A single guide RNA (sgRNA) target and protospacer adjacent motif was identified on the coding strand: 5′ CCTCGACCTCAAAACCAGCG GGG33′ with a predicted cut site 44 bp upstream of the termination codon. The sgRNA target is located at mouse chromosome 2, nucleotides 132373439–132373459 (NCBI Reference Sequence: NC_000068.7). The activity of sgRNA/Cas9 complex at the target was demonstrated by analysis of genomic DNA extracted from blastocysts that developed in in vitro culture from mouse zygotes that had been microinjected with Cas9 reagents, as described (Sakurai et al. 2014). DNA sequence analysis of PCR products obtained by amplification across the Cas9 target showed the presence of insertions/deletions (indels) in the genomic DNA due to non-homologous end joining repair of double-strand chromosome breaks induced by sgRNA/ Cas9 complexes (Fig. 1a, b). After the demonstration of effective Cas9 cleavage of the target, a donor

plasmid for homology directed repair was synthesized that included 800 bp of sequence upstream of the sgRNA target. Multiple silent coding changes were introduced in the Cas9 target to block Cas9 re-cleavage after correct repair of chromosome breaks by the donor DNA: 5′ CCTCGACt-TaAAgACatctG GcG 3′. Between the final *Prokr2* codon and termination codon a GSG linker, a T2A viral peptide, an iCre recombinase, and a bovine growth hormone polyadenylation signal (bPA) were inserted (Goodwin and Rottman 1992; Kim et al. 2011; Shimshek et al. 2002). Immediately downstream of the bPA was the endogenous Prokr2 termination codon and 797 bp of genomic sequence that comprised the 800 bp 3′ arm of homology (Fig. 1c). The sgRNA target was cloned into the plasmid pX330 (Addgene.org plasmid # 42230, a kind gift of Feng Zhang) as described (Ran et al. 2013). The circular pX330 plasmid (5 ng/μL final concentration) (Mashiko et al. 2013) and circular donor plasmid (10 ng/μL final concentration) were mixed together for microinjection. Fertilized eggs were produced by mating superovulated B6SJLF1 with B6SJLF1 males (JAX mice, stock # 100012). Pronuclear microinjection was carried out as described (Becker and Jechow 2011; Van Keuren et al. 2009). A total of 293 zygotes were microinjected, 255 surviving zygotes were transferred to B6D2F1 (JAX mice, stock # 100006) pseudopregnant female mice and 85 pups were born. Genotyping of genomic DNA extracted from tail tip biopsies was performed by PCR with primers internal and external to the DNA donor plasmid (Table 1; Fig. 1d), and confirmed by DNA sequencing analysis. Single copy integration was confirmed by PCR. Two primers pairs were used. The 5′ pair included a primer outside the 5′ arm of homology and one inside Cre recombinase. The 3′ pair included a primer outside the 3′ arm of homology and one inside Cre recombinase. Following identification of Prokr2-Cre founders, quantitative PCR of genomic iCre was performed to determine the integration events in heterozygous and homozygous mice. Interleukin 2 (*Il2* gene) was used as a random control for positive homozygosity.

Validation of Prokr2-Cre mouse models

To validate the Prokr2-Cre mouse line, we crossed the founder mice (G0 generation) with wild type mice to expand the colony, and the Cre+ offspring (G1 generation) were bred to reporter mice that express either tdTom or GFP in a Cre-dependent manner. Adult (60–80 days old) male (n = 5/group) and female (n = 6/group) mice were anesthetized with isoflurane (Fluriso, Vet One, Boise, ID, USA) and perfused transcardially with 10% buffered formalin (Sigma). Female mice were perfused on the day of diestrus after at least two normal estrous cycles. Diestrus was used as a basal condition to avoid a potential influence of different levels of sex steroids on *Prokr2* gene expression. Brains were dissected and cryoprotected overnight. Coronal sections (30-μm thickness, 5 series) were harvested on a freezing microtome and were stored in cryoprotectant solution at −20 °C. Cre-induced tdTom or GFP was assessed in series of brain sections from Prokr2-Cre reporter mice in G2 and subsequent generations. The distribution of GFP was mapped after immunohistochemistry.

Single and dual label immunohistochemistry

GFP-immunoreactivity (GFP-ir) was assessed in series of brain sections from both male and female Prokr2-Cre reporter mice. Briefly, sections were incubated in primary chicken anti-GFP antiserum (1:5000, Aves Labs, Tigard, OR, USA, cat# GFP-1020), diluted in 0.1 M

PBS + 0.25% Triton X-100 (Sigma) and 2% normal goat serum (Vector Labs., Burlingame, CA, USA), overnight on a shaker at room temperature. The next day, sections were rinsed in PBS and incubated in AlexaFluor 488-conjugated goat anti-chicken secondary antiserum (1:500, Invitrogen) for 1.5 h. Sections were mounted onto gelatin-coated slides, air dried and coverslipped with Fluoromount G™ medium (Southern Biotechnology Associates, Birmingham, AL, USA). Series of brain sections from Prokr2-Cre GFP reporter mice were also submitted to standard immunoperoxidase staining. Following incubation in anti-GFP antiserum (1:20,000), sections were incubated in biotin-conjugated donkey anti-chicken secondary antiserum (1:1000, Jackson ImmunoResearch Laboratories, West Grove, PA, USA) and avidin–biotin complex. The peroxidase reaction was performed using 3,3-diaminobenzidine tetrahydrochloride (DAB; Sigma) as a chromogen and 0.03% hydrogen peroxide dissolved in 0.1 M PBS, pH 7.4, for 3–5 min. Sections were mounted onto gelatin-coated slides, dehydrated in graded ethanol, placed in xylene for 5 min and coverslipped with DPX mounting medium (Electron Microscopy Sciences).

To assess whether Prokr2 neurons co-express gonadotropin-releasing hormone (GNRH), we used brain sections from male ($n = 4$) and female ($n = 4$) Prokr2-Cre GFP mice. Series of sections were incubated in anti-GFP antiserum (1:5000) overnight at room temperature followed by AlexaFluor-488 conjugated goat anti-chicken secondary antisera (1:500). Subsequently, sections were incubated in rabbit anti-LHRH antiserum (1:1000, Millipore, cat# AB9754) and AlexaFluor-594 conjugated secondary antiserum (1:500). Sections were mounted onto gelatin-coated slides, air-dried and coverslipped with Fluoromount.

To assess colocalization between Prokr2 and ERα, series of sections from Prokr2-Cre GFP reporter mice ($n = 3$ females) were incubated in rabbit anti-ERα antiserum (1:20,000, Upstate-Millipore, Billerica, MA, USA, cat# C1355) overnight at room temperature, followed by AlexaFluor-594 conjugated donkey anti-rabbit secondary antiserum (1:500, Invitrogen). Subsequently, sections were incubated in anti-GFP (1:5000) overnight followed by incubation in AlexaFluor-488 conjugated secondary antiserum as previously described. Sections were mounted onto gelatin-coated slides, air-dried and coverslipped with Fluoromount.

In situ hybridization histochemistry

Single-label in situ hybridization histochemistry (ISHH) was performed in brain sections of male ($n = 4$) and female ($n = 4$) C57BL/6 mice, as previously described (Donato et al. 2013; Scott et al. 2009; Zigman et al. 2006). In addition, we performed a set of ISHH in series of sections (30-μm thick) from Prokr2-Cre reporter line to evaluate if *Prokr2* gene expression was intact in the Prokr2-Cre heterozygous and homozygous mice ($n = 3$ females in diestrus and $n = 3$ males/genotype). Briefly, one series of brain sections were mounted onto SuperFrost plus slides (Fisher Scientific), air-dried overnight and fixed in 4% paraformaldehyde in DEPC-treated PBS for 20 min. Tissue was dehydrated in increasing concentrations of ethanol, cleared in xylenes, rehydrated in decreasing concentrations of ethanol, and placed in pre-warmed sodium citrate buffer, pH 6.0. Slides were microwaved for 10 min followed by dehydration in graded ethanol. The Prokr2 riboprobe was produced from mouse olfactory bulb cDNA. The following primers were used to amplify a 724 bp

sequence (mRNA (NM_144944.3): F (T3) 5′(CAG AGA TGC AAT TAA CCC TCA CTA AAG GGA GA) AGT AGG CAA GCC TCA ACC AG 3′; R (T7) 5′(CC AAG CCC TCT AAT ACG ACT CAC TAT AGG GAG A) TAC TCC CGT AGT GAG AGG GC 3′.

The Prokr2 riboprobe was generated by in vitro transcription using ^{33}P-UTP as the radioisotope. ^{33}P-labeled Prokr2 probe was diluted in hybridization solution and brain sections were hybridized overnight at 56 °C. The next day, slides were incubated in 0.002% RNAse A followed by stringency washes. Sections were dehydrated in increasing concentrations of ethanol (50–100%), air-dried and placed in X-ray film cassettes with BMR-2 film (Kodak, Rochester, NY, USA) for 2–3 days. Slides were then dipped in NTB autoradiographic emulsion (Kodak, VWR), and stored in foil-wrapped slide boxes at 4 °C for 3–4 weeks. Slides were developed with Dektel developer (Kodak, VWR, Radnor, PA, USA), counterstained with thionin, dehydrated in graded ethanol, cleared in xylenes and coverslipped with DPX.

Dual label immunohistochemistry-in situ hybridization

Dual label in situ hybridization/immunohistochemistry was performed to determine coexpression of GFP immunoreactivity with Prokr2 mRNA. Sections of Prokr2-Cre GFP mouse brains were rinsed with diethylpyrocarbonate (DEPC)-treated PBS for 1 h before being pretreated with 1% sodium borohydride (Sigma) for 15 min. After washes in DEPC-PBS, tissue was briefly rinsed in 0.1 M triethanolamine (TEA), pH 8.0 and incubated for 10 min in 0.25% acetic anhydride in 0.1 M TEA. The tissue was then rinsed in DEPC-treated 2× SSC before hybridization. The ^{33}P-labeled riboprobes were diluted to 10^6 cpm/mL in hybridization buffer and applied to the tissue. Sections were incubated overnight at 50 °C. The next day, sections were incubated in 0.002% RNase A (Roche) for 30 min at 37 °C. Sections were then submitted to stringency washes followed by immunohistochemistry for the detection of GFP-ir, as previously described, using DAB as chromogen. Sections were mounted onto SuperFrost Plus slides, dehydrated in graded ethanol and delipidated for 15 min in xylene. After washes in 100% and 95% ethanol, the tissue was air-dried, and slides were placed in X-ray film cassettes with BMR-2 film for 2–3 days. Slides were then dipped in NTB autoradiographic emulsion, and stored in foil-wrapped slide boxes at 4 °C for 2 weeks. Slides were developed with Dektel developer, dehydrated in increasing concentration of ethanol, cleared in xylenes and coverslipped with DPX.

Data analysis and production of photomicrographs

Brain sections were analyzed using an Axio Imager M2 microscope (Zeiss, Jena, Germany). The distribution of single-labeled (GFP+ or tdTomato+) neurons was initially assessed in series of the entire brain (Table 2). Brain sites showing an apparent sexually dimorphic pattern of distribution of Prokr2-Cre GFP+ cells (i.e., amigdalo-hippocampal area, posterodorsal subdivision of the medial nucleus of the amygdala, medial preoptic area, arcuate nucleus, ventrolateral subdivision of the ventromedial nucleus of the hypothalamus and parabrachial nucleus) were quantified in immunoperoxidase stained brains. Only one side from one section of each mouse brain using the same area of interest for all sections of the same nuclei was used for quantification to avoid double counting. Total number of GFP+ neurons were evaluated considering average of n = 4–5 mice/sex. The hybridization signal

was estimated by the analysis of the integrated optical density (IOD) using the ImageJ software (http://rsb.info.nih.gov/ij), as we have done before (Donato et al. 2009, 2010). Dark field photomicrographs were acquired using the same illumination and exposure time for every section. The IOD values for Prokr2 mRNA were calculated as the total IOD of a constant area subtracting the background from adjacent nuclei that did not express Prokr2 mRNA. Dual labeled neurons coexpressing GFP-ir and ERα-ir in the ventromedial nucleus of the hypothalamus were quantified. We considered cells dual labeled those with cytoplasm containing one fluorophores (AF488) and the nucleus containing the second fluorophore (AF594) detected under epifluorescence microscope. Quantification of dual labeled neurons and percentage of colocalization comparing total GFP-ir and total ERα-ir were calculated and expressed as mean ± SEM.

Photomicrographs were produced by capturing images with a digital camera (Axiocam, Zeiss) mounted directly on the microscope using the Zen software. Adobe Photoshop CS6 image-editing software was used to integrate photomicrographs into plates. For data illustration, only sharpness, contrast and brightness were adjusted. Statistical analysis was performed using GraphPad Prism 6 software. Comparison between groups (male and female) was determined by multiple t-tests. False discovery was determined by two-stage linear step-up procedure of Benjamini, Krieger and Yekutieli, with $q = 1\%$. P values and q values are presented in figure legends. Data are expressed as mean ± SEM and α values (P) <0.05 were considered significant.

Results

Production and validation of Prokr2-Cre mouse model

To generate a mouse line that expresses Cre-recombinase driven by *Prokr2* promoter (Prokr2-Cre mouse model), we built a Prokr2-Cre donor construct and identified the sgRNA by initial in vitro assessment. The activity of Cas9 at the sgRNA target was assessed by DNA extraction from blastocysts and demonstration of indels in the genomic DNA by the use of DNA sequencing (Fig. 1a, b). Prokr2-Cre DNA donor and sgRNA/Cas9 plasmids were microinjected into mouse zygotes and transferred to pseudopregnant females. Of 85 potential founders, one founder incorporated the DNA donor plasmid by correct homologous recombination identified by PCR and sequencing (Fig. 1e, f). Following qPCR analysis of genomic iCre, we found that one integration event is present per *Prokr2* allele (Fig. 1g). Two potential founders carried random integration of the DNA donor plasmid, also identified by PCR and sequencing of 5′ and 3′ homology arms. After crossing the G1 generation of Prokr2-Cre mice with reporter mice (R26-tdTom or R26-eGP), we identified Cre activity in brain nuclei previously shown to express Prokr2 mRNA (Fig. 1h–k) (Cheng et al. 2006). No differences in the pattern of Cre+ cell distribution between generations G2 and G5 were observed. Moreover, the germline transmission ratio (Mendelian ratio) is consistent with a single integration event.

We initially assessed the distribution of Cre-induced GFP in brain sites known to express high levels of *Prokr2*. We found strong and consistent Cre-induced GFP-ir in the lateral septum, the suprachiasmatic nucleus, the paraventricular nucleus of the hypothalamus and the area postrema of males and females (Fig. 2). We then compared the distribution of Cre-

induced GFP with Prokr2 mRNA by in situ hybridization. In males, high levels of Prokr2 mRNA were observed in the subventricular zone of the lateral ventricle, in olfactory nuclei, globus pallidus, amigdalo-hippocampal transition, dorsomedial hypothalamus and mammillary nuclei, as previously reported (Cheng et al. 2006). In females, however, we also found high mRNA levels in the arcuate nucleus, ventromedial nucleus and medial amygdala, and lower mRNA levels in the amigdalo-hippocampal area (Fig. 3a–i). Dense hybridization signal was observed in the pleioglial periaqueductal gray in both sexes (Fig. 3g–i).

To validate the Prokr2-Cre mouse model, we performed dual label in situ hybridization and immunohistochemistry in male and female Prokr2-Cre GFP mice. Colocalization was clearly detected in areas where Prokr2 mRNA is abundant, including the suprachiasmatic nucleus, the lateral septum, the paraventricular nucleus of the hypothalamus, the pleioglial periaqueductal gray and the area postrema (Fig. 4a–c). In brain sites with low Prokr2 mRNA expression, the degree of colocalization was variable potentially due to low mRNA levels typical of GPCRs. Cre activity alone was observed only in few nuclei of the thalamus, i.e. the ventral lateral, the ventral posteromedial and the ventral posterolateral (Fig. 4d), suggesting developmental expression of Cre and Prokr2 in these sites.

Distribution of Prokr2-Cre-induced reporter gene and Prokr2 mRNA in male and female brain

We next compared the distribution of Prokr2-Cre GFP in male and female brains (Table 2). An initial subjective analysis was performed to identify potential sexually dimorphic sites. Moderate-to-high numbers of GFP immunoreactive cells were observed in the olfactory bulb and subventricular zone of the lateral ventricle. GFP positive (GFP+) cells were observed in several areas of the cerebral cortex, specifically in the prelimbic, infralimbic, insular, retrosplenial and piriform cortex. We also found GFP-ir in the medial and lateral septum, with a higher expression in the dorsal aspect of the lateral septum. A moderate number of GFP immunoreactive cells was observed in the dentate gyrus, ventral pallidum and globus pallidus. Hippocampal regions with small numbers of GFP+ cells included CA1 and CA3.

The amygdala showed moderate to high expression of Cre-induced GFP-ir in a sexually dimorphic manner also observed for Prokr2 mRNA (Table 2). We found higher numbers of GFP positive cells and Prokr2 mRNA in the posterolateral subdivision of the medial amygdala of females and in the amigdalo-hippocampal area of males (Fig. 5A–D, Q, R). High numbers of Cre-induced GFP immunoreactive cells were observed in the anterior and medial nuclear groups of the thalamus, including the par-aventricular, paracentral, central medial nuclei, and in the lateral habenula of both sexes. Moderate numbers of GFP positive cells were found in the laterodorsal and xifoid nuclei of the thalamus, and in the medial habenula. In addition, as mentioned, we also found GFP-ir in the ventral nuclei of the thalamus, but no Prokr2 hybridization signal was observed in those areas (Table 2).

In the hypothalamus, the medial preoptic area showed a low but consistent amount of GFP+ cells in males and moderate amount in females also observed for Prokr2 mRNA (Fig. 5E–H, Q, R). High number of GFP+ cells was observed in the suprachiasmatic nucleus and parvi-cellular paraventricular nucleus of the hypothalamus, in both sexes. Moderate to high GFP-ir was detected in the dorsomedial nucleus of the hypothalamus in both sexes, whereas the

ventrolateral subdivision of the ventromedial nucleus of the hypothalamus showed moderate number of GFP+ cells and Prokr2 mRNA in females, but very little in males (Fig. 5I–L, Q, R). We also observed scattered GFP+ cells in the lateral hypothalamic area and arcuate nucleus. In the arcuate nucleus, higher number of GFP+ cells and Prokr2 mRNA were found in females (Fig. 5I–L, Q, R). In the caudal portion of the hypothalamus, GFP-ir cells were observed in the dorsal premammillary nucleus and several mammillary nuclei in both males and females (Table 2).

In the brainstem, GFP+ cells were observed in the superior colliculus, in the dorsal column and posterior aspect of the ventrolateral column of the periaqueductal gray, in the dorsal raphe, Edinger–Westphal nucleus, and medial and lateral subdivisions of the parabrachial nucleus. In the lateral parabrachial nucleus, a higher number of GFP+ cells was observed in females (Fig. 5M, N, Q, R), but this difference was not observed for Prokr2 mRNA (Fig. 5O, P). Few GFP+ cells were found in the anterior subdivision of the nucleus of the solitary tract and in the hypoglossal nucleus.

High number of GFP+ cells and Prokr2 mRNA was observed in specific circumventricular organs, including the subfornical, the subcomissural and the area postrema. Few GFP+ neurons were sporadically found in the median eminence.

Prokr2 mRNA, GnRH migration and fertility are intact in Prokr2-Cre mice

Because PROKR2 is essential for GnRH migration and fertility, we next assessed if the Cre transgene altered *Prokr2* gene expression and GnRH migration. Distribution of Prokr2 mRNA was not different between wild type and Prokr2-Cre heterozygous and homozygous mice (Fig. 6a–f). In addition, no changes in number ($P > 0.05$) and location of GnRH-ir cells, and density of fibers in the median eminence were observed (Fig. 6g–l). In agreement with previous data in wild type mice (Balasubramanian et al. 2011; Pitteloud et al. 2007), no colocalization between Prokr2-Cre GFP and GnRH immunoreactivity was detected in adult mice (Fig. 6m–o). However, we did find that several Prokr2 neurons are in close apposition with GnRH cells in the preoptic area.

We then assessed if Prokr2-Cre heterozygous and homozygous mice are fertile. Six males ($n = 3$ heterozygous and $n = 3$ homozygous) and nine females ($n = 6$ heterozygous and $n = 3$ homozygous) were evaluated from 2 to 8 months of age. The presence of one or two Cre alleles (in Prokr2-Cre heterozygous and homozygous mice) did not affect fertility in males and in females. Prokr2-Cre and wild type control mice produced an average of six pups/litter (Prokr2-Cre heterozygous, 5.75 ± 0.45 pups; homozygous, 5.92 ± 0.55 pups; wild type, 5.45 ± 0.47 pups in 2–4 fertility trials), and latency to pregnancy ranged from 1 to 5 days in average for all genotypes.

Prokr2-Cre and ERα are coexpressed in the VMHvl

Previous studies in mice have suggested that Prokr2 is regulated by changing levels of estradiol (Xiao et al. 2014). Using the Prokr2-Cre GFP mice, we assessed colocalization between ERα and GFP-ir in female brains. Little-to-no coexpression was observed in the lateral septum, medial preoptic area, anteroventral periventricular nucleus, arcuate nucleus and the posterodorsal subdivision of the medial amygdala (Fig. 7a–i). However, partial

coexpression was observed in the ventrolateral subdivision of the ventromedial nucleus of the hypothalamus (VMHvl) of females (62.3 ± 3.4% of GFP+ neurons coexpress ERα and 8.8 ± 0.9% of ERα neurons coexpress Prokr2-Cre GFP). The colocalization between Prokr2-Cre GFP and ERα was not evaluated in males due to the lack of GFP+ cells in the male. Sporadic coexpression of ERα and GFP was observed in the lateral hypothalamic area and arcuate nucleus.

Discussion

In the present study, we describe the generation and characterization of a novel preclinical model for the studies on the *Prok2/Prokr2* system using CRISPR/Cas9 technology. The Prokr2-Cre mice express iCre recombinase driven by *Prokr2* promoter, visualized using two distinct R26 reporter mice (Allen et al. 2016; Cravo et al. 2011, 2013). The expression pattern of Cre-induced reporter gene (GFP and tdTom) was compared with previous published data (Cheng et al. 2006) and our own analysis of Prokr2 mRNA distribution. Further validation of the mouse model was performed using dual label immunohistochemistry and in situ hybridization. Expression of Cre-induced reporter genes and Prokr2 mRNA were highly congruent except for several thalamic nuclei that expressed only GFP-ir in male and female adult brain. No changes in Prokr2 mRNA expression, GnRH migration or fertility were observed. Prokr2-Cre GFP is not expressed in GnRH neurons in agreement with previous studies in wild type mice (Pitteloud et al. 2007), and Prokr2/ERα colocalization was only detected in the female VMHvl.

The activity of Cas9 at the sgRNA target was initially assessed by microinjection into zygotes, culturing zygotes to the blastocyst stage and the occurrence of indels in the genomic DNA (Sakurai et al. 2014). The correct integration of the transgene DNA into the genome was obtained via homology directed repair of a chromosome break induced by CRISPR/Cas9. Whereas the probability for the integration of the transgene DNA into the genome without CRISPR/Cas9 induced DNA breaks exists, it is vanishingly small (Brinster et al. 1989). Seminal work in mouse genetics demonstrated that the efficiency of homologous recombination of microinjected transgenes in zygotes without induced DNA breaks is attained at a low frequency of 0.0094% (Brinster et al. 1989). In our study, we obtained one founder in 293 injected zygotes, representing a frequency of 0.34%, i.e. more than two orders of magnitude higher than reported in previous studies (Brinster et al. 1989). The CRISPR/Cas9 treatment of ES cells dramatically increased homologous recombination with DNA donors (Gennequin et al. 2013; Schick et al. 2016, and author’s unpublished observations). Thus, the probability that correct integration of the synthetic DNA donor molecule occurred after CRISPR/Cas9-induced chromosome break is very high and the most likely explanation for the transgene knockin in *Prokr2* sequence.

The role of Prok2/Prokr2 system in reproductive function was described after an incidental finding that mice with the deletion of *Prok2* or *Prokr2* genes had a strikingly similar phenotype to that observed in individuals with Kallmann syndrome (Matsumoto et al. 2006; Ng et al. 2005). Soon after, a series of studies reported distinct mutations in *PROK2* or *PROKR2* genes in humans diagnosed with Kallmann syndrome (Abreu et al. 2008; Canto et al. 2009; Cole et al. 2008; Leroy et al. 2008; Monnier et al. 2009; Pitteloud et al. 2007;

Sarfati et al. 2010; Sinisi et al. 2008). In both, mice and humans, the most prominent reproductive deficit caused by these genetic mutations is the arrest of GnRH neurons in the cribiform plate and disruption of their migratory path from the olfactory pla-code to the hypothalamus (and medial septum in rodents) (Cariboni et al. 2007; Norgren and Lehman 1991; Pitteloud et al. 2007; Wierman et al. 2011). The lack of GnRH migration disrupts sexual maturation and fertility in mice and humans, revealing an incontestable role for *Prok2/ PROK2* and *Prokr2/PROKR2* in reproductive function. Whereas these findings represented a breakthrough to the field, a series of questions remained unanswered (Balasubramanian et al. 2011). For example, the mechanisms by which PROK2 promotes GnRH neuronal migration, the neuroendocrine action of PROK2/PROKR2 system in the reproductive and other endocrine axes, and the role of other Prokr2 neuronal populations are still poorly understood. Due to the widespread distribution of Prokr2 neurons, the lack of sophisticated mouse models and experimental tools has precluded a better understanding and dissection of the PROK2/PROKR2 systems. The use of global knockout mouse and pharmacological approaches has generated important but sometimes imprecise or ambiguous data.

The recent development of molecular techniques and the use of genetic mouse models have allowed an impressive advance in our understanding of brain circuitry and physiology. Conditional gene knockouts, conditional gene re-expression, molecular mapping using viro-genetic and remote activation or inhibition of specific neural circuits using chemo- or optogenetic control have revolutionized the way scientific knowledge has advanced (Cravo et al. 2011, 2013; Elias 2014; Klockener et al. 2011; Krashes et al. 2013; Lam et al. 2011; Sadagurski et al. 2012; Simonds et al. 2014; Sternson and Roth 2014; Wang et al. 2014). The downside, however, has been the time and cost to produce the genetically engineered mouse models to perform the crucial experiments. With the development of the CRISPR/Cas9 technology, these issues are minimized. The RNA-guided endonuclease Cas9 from streptococcus pyrogenes has been successfully used for genetic manipulations in experimental animal models (Lee and Lloyd 2014; Mashiko et al. 2014; Platt et al. 2014; Wang et al. 2013). The Prokr2-Cre mouse was generated by inducing a chromosome break near the *Prokr2* termination codon followed by homology directed repair of the break and insertion of iCre sequence.

Following the identification of a Prokr2-Cre founder, the mouse was bred with two distinct lines of Cre-induced reporter genes (GFP and tdTom) to evaluate the efficiency of loxP recombination (Allen et al. 2016; Borges et al. 2016; Cravo et al. 2011, 2013). In both cases, we found a similar distribution of labeled cells throughout the brain. We chose to perform the validation of the mouse model, i.e., the colocalization of Cre-induced reporter gene and Prokr2 mRNA, using the Prokr2-Cre GFP mice due to the higher efficiency obtained following the in situ hybridization procedure. Whereas the coexpression of Cre induced reporter genes and Prokr2 mRNA were highly congruent, several thalamic nuclei (mostly the ventral group) displayed cells positive to GFP (in single or dual label procedures) or tdTom (auto-fluorescence). This finding suggests that neurons in these areas expressed *Prokr2* earlier in development and the expression was silenced in adult life. Alternatively, it is also possible that Prokr2 mRNA is very low in these sites, undetectable using ISHH.

Developmental fate mapping with Prokr2-Cre mice can be made in the future to address these questions.

The distribution of Prokr2-Cre expressing neurons in males and females were mapped using GFP immunoperoxidase and tdTomato auto-fluorescence in independent cohorts. The sexually dimorphic pattern of Prokr2-Cre cells was evident in several brain regions. As reported by others (Xiao et al. 2014), higher numbers of Prokr2-Cre neurons were found in the preoptic area of females, but virtually no coexpression of ERα was observed in that site, suggesting that a direct effect of estradiol via ERα is not the main mechanism for estrogen action. We did find that Prokr2-Cre GFP and ERα are coexpressed in the female, not in the male, VMHvl, a hypothalamic nucleus associated with female sexual behavior (Flanagan-Cato 2011; Musatov et al. 2006). Given the reported role of Prokr2 in estrous cycling (Xiao et al. 2014), further investigations on the specific neuronal subpopulations and mechanisms associated with ERα and Prokr2 signaling are warranted.

The sexually dimorphic pattern of Prokr2-Cre distribution in the amygdala is of great interest. The medial amygdala densely expresses sex steroids receptor and is a secondary relay of the vomeronasal system (Rasia-Filho et al. 1991; Scalia and Winans 1975; Simerly et al. 1990; Wood and Coolen 1997; Wood and Newman 1995). Those neurons are activated (Fos-ir) following pheromone exposure and sexual behavior, and electrochemical stimulation of the medial amygdala increases LH secretion (Beltramino and Taleisnik 1978; Bressler and Baum 1996; Coolen et al. 1996; Kollack-Walker and Newman 1995; Veening et al. 2005). Studies suggest the existence of a topographic distribution of neurons associated with segregation between conspecific (socially relevant) and heterospecific (socially irrelevant) chemosensory stimuli (Meredith and Westberry 2004). The Prokr2-Cre mouse model will be useful to examine the role of Prokr2 cells in these aspects of the reproductive function and the motivated behaviors in a sexually dimorphic manner.

A moderate to high expression of Prokr2-Cre was observed in the PVH of both males and females. The PVH is a complex structure comprised of neurons associated with neuroendocrine, autonomic and behavioral controls (Biag et al. 2012; Garfield et al. 2015; Sawchenko and Arias 1995; Sawchenko et al. 1984, 1996; Shah et al. 2014; Swanson and Kuypers 1980; Swanson and Sawchenko 1980). Interestingly, studies have reported that Prokr2-null mice show reduced pituitary gland size, and that individuals with *PROKR2* loss-of-function mutation display combined pituitary hormone deficiency (CPHD) (McCabe et al. 2013; Raivio et al. 2012). In addition to low levels of LH and FSH, these individuals also show low levels of growth hormone (GH), vasopressin (AVP), thyrotropin-stimulating hormone (TSH) and adrenocorticotropic hormone (ACTH) (Asakura et al. 2015; Correa et al. 2015; Raivio et al. 2012; Reynaud et al. 2012). The Prokr2-Cre mice will allow for the dissociation between the effects of releasing factors from hypothalamic neurosecretory neurons, including the PVH, and the endocrine secretion from the pituitary gland on the hypopituitarism and CPHD observed in *Prokr2/PROKR2* gene mutation.

Prok2/Prokr2 cells have been also linked to other physiological systems. This is not surprising considering the widespread distribution of *Prokr2* expression in the brain (Cheng et al. 2006). Circadian regulation, energy balance (food intake and energy expenditure),

glucose homeostasis, stress response, cardiovascular regulation and locomotor activity are among the complex systems associated with PROKR2 function (Abreu et al. 2010; Balasubramanian et al. 2011; Cheng et al. 2002, 2005; Gardiner et al. 2010; Martin et al. 2011; Prosser et al. 2007; Zhou and Cheng 2005). Therefore, the Prokr2-Cre mouse represents a crucial preclinical model for the understanding of the neural circuitry and molecular mechanisms associated with Kallmann syndrome, GnRH neuronal migration, hypothalamic control of the reproductive function and many other physiological systems.

Acknowledgments

We would like to thank Drs. Crowley and Balasubramanian (MGH, Harvard University, Boston) for insightful discussions and encouragement for the production of this mouse model. We also thank Susan Allen for the expert technical assistance. We acknowledge Wanda Filipiak and Galina Gavrilina for the preparation of transgenic mice and the Transgenic Animal Model Core of the University of Michigan's Biomedical Research Core Facilities. Core support was provided by the following NIH Grants: P30CA046592, DK34933 (University of Michigan Gut Peptide Research Center), P30DK08194 (University of Michigan George M. O'Brien Renal Core Center). Research support was provided by NIH HD69702 Grant (to C.F.E.) and T32 fellowship (to H.S.).

References

Abreu AP, et al. Loss-of-function mutations in the genes encoding prokineticin-2 or prokineticin receptor-2 cause autosomal recessive Kallmann syndrome. J Clin Endocrinol Metab. 2008; 93:4113–4118. DOI: 10.1210/jc.2008-0958 [PubMed: 18682503]

Abreu AP, Kaiser UB, Latronico AC. The role of prokineticins in the pathogenesis of hypogonadotropic hypogonadism. Neuroendocrinology. 2010; 91:283–290. DOI: 10.1159/000308880 [PubMed: 20502053]

Abreu AP, Noel SD, Xu S, Carroll RS, Latronico AC, Kaiser UB. Evidence of the importance of the first intracellular loop of prokineticin receptor 2 in receptor function. Mol Endocrinol. 2012; 26:1417–1427. DOI: 10.1210/me.2012-1102 [PubMed: 22745195]

Allen SJ, Garcia-Galiano D, Borges BC, Burger LL, Boehm U, Elias CF. Leptin receptor null mice with re-expression of LepR in GnRH-R expressing cells display elevated FSH levels but remain in a prepubertal state. Am J Physiol Regul Integr Comp Physiol. 2016; 00529:02015. doi: 10.1152/ajpregu.00529.2015

Asakura Y, et al. Combined pituitary hormone deficiency with unique pituitary dysplasia and morning glory syndrome related to a heterozygous PROKR2 mutation. Clin Pediatr Endocrinol. 2015; 24:27–32. DOI: 10.1297/cpe.24.27 [PubMed: 25678757]

Balasubramanian R, Plummer L, Sidis Y, Pitteloud N, Martin C, Zhou QY, Crowley WF Jr. The puzzles of the prokineticin 2 pathway in human reproduction. Mol Cell Endocrinol. 2011; 346:44–50. DOI: 10.1016/j.mce.2011.05.040 [PubMed: 21664414]

Becker, K., Jechow, B. Generation of transgenic mice by pronuclear microinjection. In: Pease, S., Saunders, TL., editors. Advanced protocols for animal transgenesis: an ISTT manual. Springer; Berlin: 2011. p. 99-116.

Beltramino C, Taleisnik S. Facilitatory and inhibitory effects of electrochemical stimulation of the amygdala on the release of luteinizing hormone. Brain Res. 1978; 144:95–107. [PubMed: 565243]

Biag J, et al. Cyto- and chemoarchitecture of the hypothalamic paraventricular nucleus in the C57BL/6J male mouse: a study of immunostaining and multiple fluorescent tract tracing. J Comp Neurol. 2012; 520:6–33. DOI: 10.1002/cne.22698 [PubMed: 21674499]

Borges BC, Garcia-Galiano D, Rorato R, Elias LL, Elias CF. PI3K p110beta subunit in leptin receptor expressing cells is required for the acute hypophagia induced by endotoxemia. Mol Metab. 2016; 5:379–391. DOI: 10.1016/j.molmet.2016.03.003 [PubMed: 27257598]

Bressler SC, Baum MJ. Sex comparison of neuronal Fos immunoreactivity in the rat vomeronasal projection circuit after chemosensory stimulation. Neuroscience. 1996; 71:1063–1072. [PubMed: 8684610]

Brinster RL, Braun RE, Lo D, Avarbock MR, Oram F, Palmiter RD. Targeted correction of a major histocompatibility class II E alpha gene by DNA microinjected into mouse eggs. Proc Natl Acad Sci USA. 1989; 86:7087–7091. [PubMed: 2506546]

Canto P, Munguia P, Soderlund D, Castro JJ, Mendez JP. Genetic analysis in patients with Kallmann syndrome: coexistence of mutations in prokineticin receptor 2 and KAL1. J Androl. 2009; 30:41–45. DOI: 10.2164/jandrol.108.005314 [PubMed: 18723471]

Cariboni A, Maggi R, Parnavelas JG. From nose to fertility: the long migratory journey of gonadotropin-releasing hormone neurons. Trends Neurosci. 2007; 30:638–644. DOI: 10.1016/j.tins.2007.09.002 [PubMed: 17981344]

Cheng MY, et al. Prokineticin 2 transmits the behavioural circadian rhythm of the suprachiasmatic nucleus. Nature. 2002; 417:405–410. DOI: 10.1038/417405a [PubMed: 12024206]

Cheng MY, Bittman EL, Hattar S, Zhou QY. Regulation of prokineticin 2 expression by light and the circadian clock. BMC Neurosci. 2005; 6:17.doi: 10.1186/1471-2202-6-17 [PubMed: 15762991]

Cheng MY, Leslie FM, Zhou Q-Y. Expression of prokineticins and their receptors in the adult mouse brain. J Comp Neurol. 2006; 498:796–809. DOI: 10.1002/cne.21087 [PubMed: 16927269]

Cole LW, et al. Mutations in prokineticin 2 and prokineticin receptor 2 genes in human gonadotrophin-releasing hormone deficiency: molecular genetics and clinical spectrum. J Clin Endocrinol Metab. 2008; 93:3551–3559. DOI: 10.1210/jc.2007-2654 [PubMed: 18559922]

Cong L, et al. Multiplex genome engineering using CRISPR/ Cas systems. Science. 2013; 339:819–823. DOI: 10.1126/science.1231143 [PubMed: 23287718]

Coolen LM, Peters HJ, Veening JG. Fos immunoreactivity in the rat brain following consummatory elements of sexual behavior: a sex comparison. Brain Res. 1996; 738:67–82. [PubMed: 8949929]

Correa FA, et al. FGFR1 and PROKR2 rare variants found in patients with combined pituitary hormone deficiencies. Endocr Connect. 2015; 4:100–107. DOI: 10.1530/ec-15-0015 [PubMed: 25759380]

Cravo RM, et al. Characterization of Kiss1 neurons using transgenic mouse models. Neuroscience. 2011; 173:37–56. DOI: 10.1016/j.neuroscience.2010.11.022 [PubMed: 21093546]

Cravo RM, et al. Leptin signaling in Kiss1 neurons arises after pubertal development. PLoS One. 2013; 8:e58698.doi: 10.1371/journal.pone.0058698 [PubMed: 23505551]

Dodé C, et al. Kallmann syndrome: mutations in the genes encoding prokineticin-2 and prokineticin receptor-2. PLoS Genet. 2006; 2:e175.doi: 10.1371/journal.pgen.0020175 [PubMed: 17054399]

Donato J Jr, et al. The ventral premammillary nucleus links fasting-induced changes in leptin levels and coordinated luteinizing hormone secretion. J Neurosci. 2009; 29:5240–5250. DOI: 10.1523/jneurosci.0405-09.2009 [PubMed: 19386920]

Donato J Jr, Frazao R, Fukuda M, Vianna CR, Elias CF. Leptin induces phosphorylation of neuronal nitric oxide synthase in defined hypothalamic neurons. Endocrinology. 2010; 151:5415–5427. DOI: 10.1210/en.2010-0651 [PubMed: 20881244]

Donato J Jr, Lee C, Ratra DV, Franci CR, Canteras NS, Elias CF. Lesions of the ventral premammillary nucleus disrupt the dynamic changes in Kiss1 and GnRH expression characteristic of the proestrusestrus transition. Neuroscience. 2013; 241:67–79. DOI: 10.1016/j.neuroscience.2013.03.013 [PubMed: 23518222]

Elias CF. A critical view of the use of genetic tools to unveil neural circuits: the case of leptin action in reproduction. Am J Physiol Regul Integr Comp Physiol. 2014; 306:R1–R9. DOI: 10.1152/ajpregu.00444.2013 [PubMed: 24196667]

Flanagan-Cato LM. Sex differences in the neural circuit that mediates female sexual receptivity. Front Neuroendocrinol. 2011; 32:124–136. DOI: 10.1016/j.yfrne.2011.02.008 [PubMed: 21338620]

Gardiner JV, et al. Prokineticin 2 is a hypothalamic neuropeptide that potently inhibits food intake. Diabetes. 2010; 59:397–406. DOI: 10.2337/db09-1198 [PubMed: 19933997]

Garfield AS, et al. A neural basis for melanocortin-4 receptor-regulated appetite. Nat Neurosci. 2015; 18:863–871. DOI: 10.1038/nn.4011 [PubMed: 25915476]

Gennequin B, Otte DM, Zimmer A. CRISPR/Cas-induced double-strand breaks boost the frequency of gene replacements for humanizing the mouse Cnr2 gene. Biochem Biophys Res Commun. 2013; 441:815–819. DOI: 10.1016/j.bbrc.2013.10.138 [PubMed: 24211574]

Goodwin EC, Rottman FM. The 3′-flanking sequence of the bovine growth hormone gene contains novel elements required for efficient and accurate polyadenylation. J Biol Chem. 1992; 267:16330–16334. [PubMed: 1644817]

Hu WP, Li JD, Zhang C, Boehmer L, Siegel JM, Zhou QY. Altered circadian and homeostatic sleep regulation in prokineticin 2-deficient mice. Sleep. 2007; 30:247–256. [PubMed: 17425220]

Kim JH, et al. High cleavage efficiency of a 2A peptide derived from porcine teschovirus-1 in human cell lines, zebrafish and mice. PLoS One. 2011; 6:e18556.doi: 10.1371/journal.pone.0018556 [PubMed: 21602908]

Klockener T, et al. High-fat feeding promotes obesity via insulin receptor/PI3K-dependent inhibition of SF-1 VMH neurons. Nat Neurosci. 2011; 14:911–918. DOI: 10.1038/nn.2847 [PubMed: 21642975]

Kollack-Walker S, Newman SW. Mating and agonistic behavior produce different patterns of Fos immunolabeling in the male Syrian hamster brain. Neuroscience. 1995; 66:721–736. [PubMed: 7644033]

Krashes MJ, Shah BP, Koda S, Lowell BB. Rapid versus delayed stimulation of feeding by the endogenously released AgRP neuron mediators GABA, NPY, and AgRP. Cell Metab. 2013; 18:588–595. DOI: 10.1016/j.cmet.2013.09.009 [PubMed: 24093681]

Lam DD, et al. Leptin does not directly affect CNS serotonin neurons to influence appetite. Cell Metab. 2011; 13:584–591. DOI: 10.1016/j.cmet.2011.03.016 [PubMed: 21531340]

Lee AY, Lloyd KC. Conditional targeting of Ispd using paired Cas9 nickase and a single DNA template in mice. FEBS Open Bio. 2014; 4:637–642. DOI: 10.1016/j.fob.2014.06.007

Leroy C, et al. Biallelic mutations in the prokineticin-2 gene in two sporadic cases of Kallmann syndrome. Eur J Hum Genet. 2008; 16:865–868. DOI: 10.1038/ejhg.2008.15 [PubMed: 18285834]

Li JD, et al. Attenuated circadian rhythms in mice lacking the prokineticin 2 gene. J Neurosci. 2006; 26:11615–11623. DOI: 10.1523/JNEUROSCI.3679-06.2006 [PubMed: 17093083]

Lin DC-H, Bullock CM, Ehlert FJ, Chen J-L, Tian H, Zhou Q-Y. Identification and molecular characterization of two closely related G protein-coupled receptors activated by proki-neticins/ endocrine gland vascular endothelial growth factor. J Biol Chem. 2002; 277:19276–19280. DOI: 10.1074/jbc.M202139200 [PubMed: 11886876]

Mali P, et al. RNA-guided human genome engineering via Cas9. Science. 2013; 339:823–826. DOI: 10.1126/science.1232033 [PubMed: 23287722]

Martin C, et al. The role of the prokineticin 2 pathway in human reproduction: evidence from the study of human and murine gene mutations. Endocr Rev. 2011; 32:225–246. DOI: 10.1210/er.2010-0007 [PubMed: 21037178]

Mashiko D, Fujihara Y, Satouh Y, Miyata H, Isotani A, Ikawa M. Generation of mutant mice by pronuclear injection of circular plasmid expressing Cas9 and single guided RNA. Sci Rep. 2013; 3:3355.doi: 10.1038/srep03355 [PubMed: 24284873]

Mashiko D, et al. Feasibility for a large scale mouse mutagenesis by injecting CRISPR/Cas plasmid into zygotes. Dev Growth Differ. 2014; 56:122–129. DOI: 10.1111/dgd.12113 [PubMed: 24372541]

Masuda Y, et al. Isolation and identification of EG-VEGF/ prokineticins as cognate ligands for two orphan G-protein-coupled receptors. Biochem Biophys Res Commun. 2002; 293:396–402. DOI: 10.1016/S0006-291X(02)00239-5 [PubMed: 12054613]

Matsumoto S-I, et al. Abnormal development of the olfactory bulb and reproductive system in mice lacking prokineticin receptor PKR2. Proc Natl Acad Sci USA. 2006; 103:4140–4145. DOI: 10.1073/pnas.0508881103 [PubMed: 16537498]

McCabe MJ, et al. Variations in PROKR2, but not PROK2, are associated with hypopituitarism and septo-optic dysplasia. J Clin Endocrinol Metab. 2013; 98:E547–E557. DOI: 10.1210/jc.2012-3067 [PubMed: 23386640]

Meredith M, Westberry JM. Distinctive responses in the medial amygdala to same-species and different-species pheromones. J Neurosci. 2004; 24:5719–5725. [PubMed: 15215294]

Monnier C, et al. PROKR2 missense mutations associated with Kallmann syndrome impair receptor signalling activity. Hum Mol Genet. 2009; 18:75–81. DOI: 10.1093/hmg/ddn318 [PubMed: 18826963]

Musatov S, Chen W, Pfaff DW, Kaplitt MG, Ogawa S. RNAi-mediated silencing of estrogen receptor alpha in the ventromedial nucleus of hypothalamus abolishes female sexual behaviors. Proc Natl Acad Sci USA. 2006; 103:10456–10460. [PubMed: 16803960]

Ng KL, Li J-D, Cheng MY, Leslie FM, Lee AG, Zhou Q-Y. Dependence of olfactory bulb neurogenesis on prokineticin 2 signaling. Science. 2005; 308:1923–1927. DOI: 10.1126/science.1112103 [PubMed: 15976302]

Norgren RB, Lehman MN. Neurons that migrate from the olfactory epithelium in the chick express luteinizing hormone-releasing hormone. Endocrinology. 1991; 128:1676–1678. DOI: 10.1210/endo-128-3-1676 [PubMed: 1999180]

Pitteloud N, et al. Loss-of-function mutation in the prokineticin 2 gene causes Kallmann syndrome and normosmic idiopathic hypogonadotropic hypogonadism. Proc Natl Acad Sci. 2007; 104:17447–17452. DOI: 10.1073/pnas.0707173104 [PubMed: 17959774]

Platt RJ, et al. CRISPR-Cas9 knockin mice for genome editing and cancer modeling. Cell. 2014; 159:440–455. DOI: 10.1016/j.cell.2014.09.014 [PubMed: 25263330]

Prosser HM, Bradley A, Chesham JE, Ebling FJ, Hastings MH, Maywood ES. Prokineticin receptor 2 (Prokr2) is essential for the regulation of circadian behavior by the suprachiasmatic nuclei. Proc Natl Acad Sci USA. 2007; 104:648–653. DOI: 10.1073/pnas.0606884104 [PubMed: 17202262]

Raivio T, et al. Genetic overlap in Kallmann syndrome, combined pituitary hormone deficiency, and septo-optic dysplasia. J Clin Endocrinol Metab. 2012; 97:E694–E699. DOI: 10.1210/jc.2011-2938 [PubMed: 22319038]

Ran FA, Hsu PD, Wright J, Agarwala V, Scott DA, Zhang F. Genome engineering using the CRISPR-Cas9 system. Nat Protoc. 2013; 8:2281–2308. http://www.nature.com/nprot/journal/v8/n11/abs/nprot.2013.143.html#supplementary-information. DOI: 10.1038/nprot.2013.143 [PubMed: 24157548]

Rasia-Filho AA, Peres TM, Cubilla-Gutierrez FH, Lucion AB. Effect of estradiol implanted in the corticomedial amygdala on the sexual behavior of castrated male rats. Braz J Med Biol Res. 1991; 24:1041–1049. [PubMed: 1797257]

Reynaud R, et al. PROKR2 variants in multiple hypopituitarism with pituitary stalk interruption. J Clin Endocrinol Metab. 2012; 97:E1068–E1073. DOI: 10.1210/jc.2011-3056 [PubMed: 22466334]

Sadagurski M, et al. IRS2 signaling in LepR-b neurons suppresses FoxO1 to control energy balance independently of leptin action. Cell Metab. 2012; 15:703–712. DOI: 10.1016/j.cmet.2012.04.011 [PubMed: 22560222]

Sakurai T, Watanabe S, Kamiyoshi A, Sato M, Shindo T. A single blastocyst assay optimized for detecting CRISPR/Cas9 system-induced indel mutations in mice. BMC Biotechnol. 2014; 14:69.doi: 10.1186/1472-6750-14-69 [PubMed: 25042988]

Sarfati J, Dode C, Young J. Kallmann syndrome caused by mutations in the PROK2 and PROKR2 genes: pathophysiology and genotype-phenotype correlations. Front Horm Res. 2010; 39:121–132. DOI: 10.1159/000312698 [PubMed: 20389090]

Sawchenko PE, Arias C. Evidence for short-loop feedback effects of ACTH on CRF and vasopressin expression in parvocellular neurosecretory neurons. J Neuroendocrinol. 1995; 7:721–731. [PubMed: 8547950]

Sawchenko PE, Swanson LW, Vale WW. Corticotropin-releasing factor: co-expression within distinct subsets of oxytocin-, vasopressin-, and neurotensin-immunoreactive neurons in the hypothalamus of the male rat. J Neurosci. 1984; 4:1118–1129. [PubMed: 6609226]

Sawchenko PE, Brown ER, Chan RK, Ericsson A, Li HY, Roland BL, Kovacs KJ. The paraventricular nucleus of the hypothalamus and the functional neuroanatomy of visceromotor responses to stress. Prog Brain Res. 1996; 107:201–222. [PubMed: 8782521]

Scalia F, Winans SS. The differential projections of the olfactory bulb and accessory olfactory bulb in mammals. J Comp Neurol. 1975; 161:31–55. [PubMed: 1133226]

Schick JA, et al. CRISPR-Cas9 enables conditional mutagenesis of challenging loci. Sci Rep. 2016; 6:32326.doi: 10.1038/srep32326 [PubMed: 27580957]

Scott MM, Lachey JL, Sternson SM, Lee CE, Elias CF, Friedman JM, Elmquist JK. Leptin targets in the mouse brain. J Comp Neurol. 2009; 514:518–532. DOI: 10.1002/cne.22025 [PubMed: 19350671]

Shah BP, et al. MC4R-expressing glutamatergic neurons in the paraventricular hypothalamus regulate feeding and are synaptically connected to the parabrachial nucleus. Proc Natl Acad Sci USA. 2014; 111:13193–13198. DOI: 10.1073/pnas.1407843111 [PubMed: 25157144]

Shimshek DR, et al. Codon-improved Cre recombinase (iCre) expression in the mouse. Genesis. 2002; 32:19–26. [PubMed: 11835670]

Simerly RB, Chang C, Muramatsu M, Swanson LW. Distribution of androgen and estrogen receptor mRNA-containing cells in the rat brain: an in situ hybridization study. J Comp Neurol. 1990; 294:76–95. [PubMed: 2324335]

Simonds SE, et al. Leptin mediates the increase in blood pressure associated with obesity. Cell. 2014; 159:1404–1416. DOI: 10.1016/j.cell.2014.10.058 [PubMed: 25480301]

Sinisi AA, et al. Homozygous mutation in the prokineticin-receptor2 gene (Val274Asp) presenting as reversible Kallmann syndrome and persistent oligozoospermia: case report. Hum Reprod. 2008; 23:2380–2384. DOI: 10.1093/humrep/den247 [PubMed: 18596028]

Soga T, et al. Molecular cloning and characterization of prokineticin receptors. Biochem Biophys Acta. 2002; 1579:173–179. [PubMed: 12427552]

Sternson SM, Roth BL. Chemogenetic tools to interrogate brain functions. Annu Rev Neurosci. 2014; 37:387–407. DOI: 10.1146/annurev-neuro-071013-014048 [PubMed: 25002280]

Swanson LW, Kuypers HG. The paraventricular nucleus of the hypothalamus: cytoarchitectonic subdivisions and organization of projections to the pituitary, dorsal vagal complex, and spinal cord as demonstrated by retrograde fluorescence double-labeling methods. J Comp Neurol. 1980; 194:555–570. [PubMed: 7451682]

Swanson LW, Sawchenko PE. Paraventricular nucleus: a site for the integration of neuroendocrine and autonomic mechanisms. Neuroendocrinology. 1980; 31:410–417. [PubMed: 6109264]

Van Keuren ML, Gavrilina GB, Filipiak WE, Zeidler MG, Saunders TL. Generating transgenic mice from bacterial artificial chromosomes: transgenesis efficiency, integration and expression outcomes. Transgenic Res. 2009; 18:769–785. DOI: 10.1007/s11248-009-9271-2 [PubMed: 19396621]

Veening JG, Coolen LM, de Jong TR, Joosten HW, de Boer SF, Koolhaas JM, Olivier B. Do similar neural systems subserve aggressive and sexual behaviour in male rats? Insights from c-Fos and pharmacological studies. Eur J Pharmacol. 2005; 526:226–239. [PubMed: 16263109]

Wang H, Yang H, Shivalila CS, Dawlaty MM, Cheng AW, Zhang F, Jaenisch R. One-step generation of mice carrying mutations in multiple genes by CRISPR/Cas-mediated genome engineering. Cell. 2013; 153:910–918. DOI: 10.1016/j.cell.2013.04.025 [PubMed: 23643243]

Wang L, et al. Pten deletion in RIP-Cre neurons protects against type 2 diabetes by activating the anti-inflammatory reflex. Nat Med. 2014; 20:484–492. DOI: 10.1038/nm.3527 [PubMed: 24747746]

Wierman ME, Kiseljak-Vassiliades K, Tobet S. Gonadotropin-releasing hormone (GnRH) neuron migration: initiation, maintenance and cessation as critical steps to ensure normal reproductive function. Front Neuroendocrinol. 2011; 32:43–52. DOI: 10.1016/j.yfrne.2010.07.005 [PubMed: 20650288]

Wood RI, Coolen LM. Integration of chemosensory and hormonal cues is essential for sexual behaviour in the male Syrian hamster: role of the medial amygdaloid nucleus. Neuroscience. 1997; 78:1027–1035. [PubMed: 9174071]

Wood RI, Newman SW. Integration of chemosensory and hormonal cues is essential for mating in the male Syrian hamster. J Neurosci. 1995; 15:7261–7269. [PubMed: 7472480]

Xiao L, et al. Signaling role of prokineticin 2 on the estrous cycle of female mice. PLoS One. 2014; 9:e90860.doi: 10.1371/journal.pone.0090860 [PubMed: 24633064]

Zhou QY, Cheng MY. Prokineticin 2 and circadian clock output. FEBS J. 2005; 272:5703–5709. DOI: 10.1111/j.1742-4658.2005.04984.x [PubMed: 16279936]

Zigman JM, Jones JE, Lee CE, Saper CB, Elmquist JK. Expression of ghrelin receptor mRNA in the rat and the mouse brain. J Comp Neurol. 2006; 494:528–548. DOI: 10.1002/cne.20823 [PubMed: 16320257]

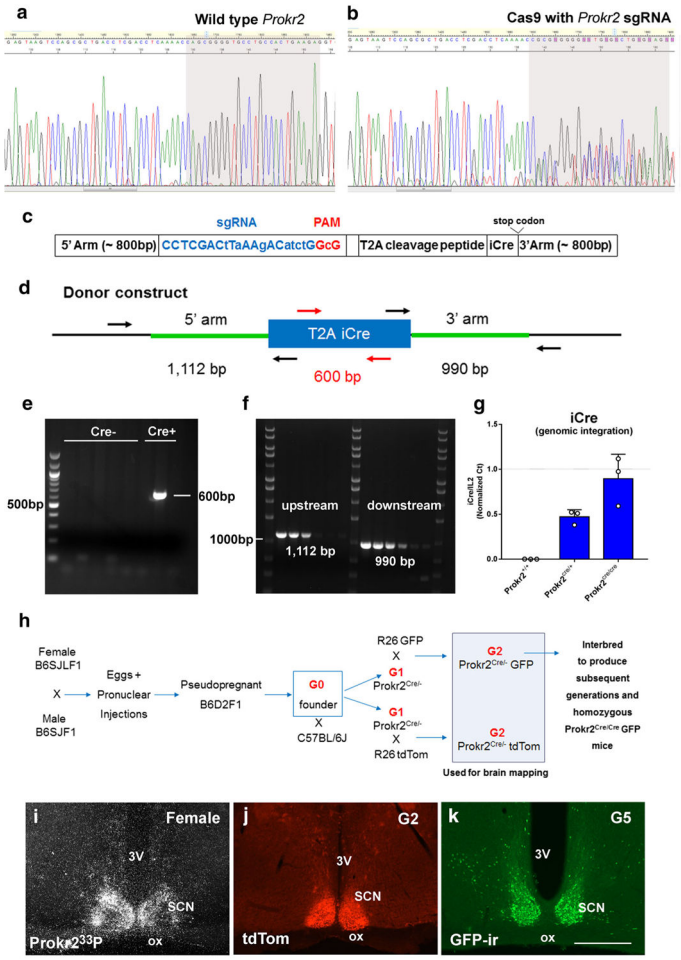

Fig. 1.

Generation of the Prokr2-Cre mouse line. **a**, **b** Chromatogram of DNA sequence from PCR products obtained by amplification across the Cas9 target shows the presence of indels in the genomic DNA due to non-homologous end joining repair of double-strand chromosome breaks induced by sgRNA/Cas9 complexes (**b**). **c**, **d** Schematic diagrams of the Prokr2-Cre donor construct used in the generation of Prokr2-Cre mouse model (**c**) showing the position of primers used to identify Prokr2-Cre founders (**d**). Note the position of the primers outside the homology arms to control for the correct insertion of Cre into the genome. **e**, **f** Images of agarose gels showing genotyping data of potential founders for the integration of Cre (**e**) and correct insertion of Cre sequence downstream of *Prokr2* gene (*different bands* temperature gradient, **f**). **g** *Bar graphs* showing quantification analysis of iCre integration events using *Il2* gene as a random positive control. Note that iCre and *Il2* are found in the same dosage in $Prokr2^{Cre/Cre}$ mice, and iCre is reduced to half the amount of *Il2* in $Prokr2^{Cre/+}$ mice. **h** Schematic illustration of the breeding strategy used to obtain Prokr2-Cre reporter mice and Prokr2-Cre homozygous mice. **i**–**k** Digital images showing the distribution of Prokr2 mRNA (wild type mouse), Prokr2-Cre tdTomato and Prokr2-Cre GFP in the suprachiasmatic nucleus (SCN) in female brains (P60–80 days of age). *3V* third ventricle, *G2* generation 2, *G5* generation 5, *ox* optic chiasm. *Scale bar* 200 μm

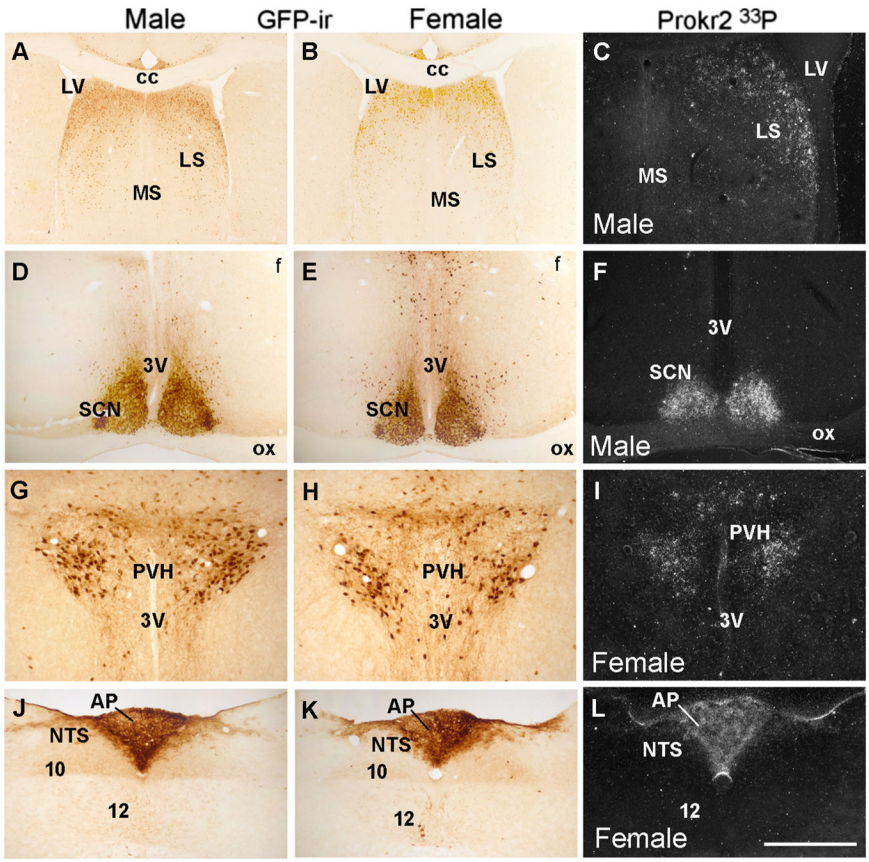

Fig. 2.

Distribution of Prokr2-Cre GFP neurons and Prokr2 mRNA in male and female brain (G3 generation, P60–80 days of age). **A**–**L** Bright- and dark-field images showing distribution of GFP immunoreactive cells (GFP-ir) and Prokr2 mRNA in male (**A**, **C**, **D**, **F**, **G**, **J**) and female (**B**, **E**, **G**, **I**–**K**) brains. *3V* third ventricle, *10* motor nucleus of the vagus nerve, *12* hypoglossal nucleus, *AP* area postrema, *cc* corpus callosum, *f* fornix, *LS* lateral septum, *LV* lateral ventricle, *MS* medial septum, *NTS* nucleus of the solitary tract, *ox* optic chiasm, *PVH* paraventricular nucleus of the hypothalamus, *SCN* suprachiasmatic nucleus. *Scale bar* **A**, **B** 400 μm, **C**–**L** 200 μm

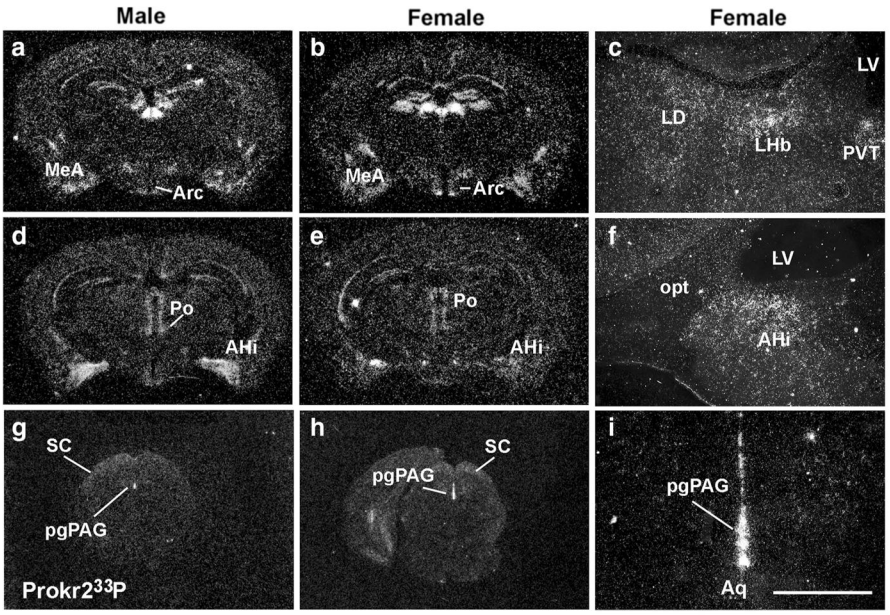

Fig. 3.

Distribution of Prokr2 mRNA in male and female brains. **a**–**i** Dark field images showing distribution of Prokr2 mRNA (hybridization signal observed as silver grains) in male (**a**, **d**, **g**) and female (**b**, **c**, **e**, **f**, **h**, **i**) brains. *AHi* amygdalohippocampal area, *Aq* aqueduct, *Arc* arcuate nucleus, *LD* laterodorsal nucleus of the thalamus, *LHb* lateral habenula, *LV* lateral ventricle, *MeA* medial nucleus of the amygdala, *opt* optic tract, *pgPAG* pleioglial periaqueductal gray, *Po* posterior hypothalamus, *PVT* paraventricular nucleus of the thalamus, *SC* superior colliculus. *Scale bar* **a**, **b**, **d**, **e**, **g**, **h** 2 mm; **c**, **f**, **i** 200 μm

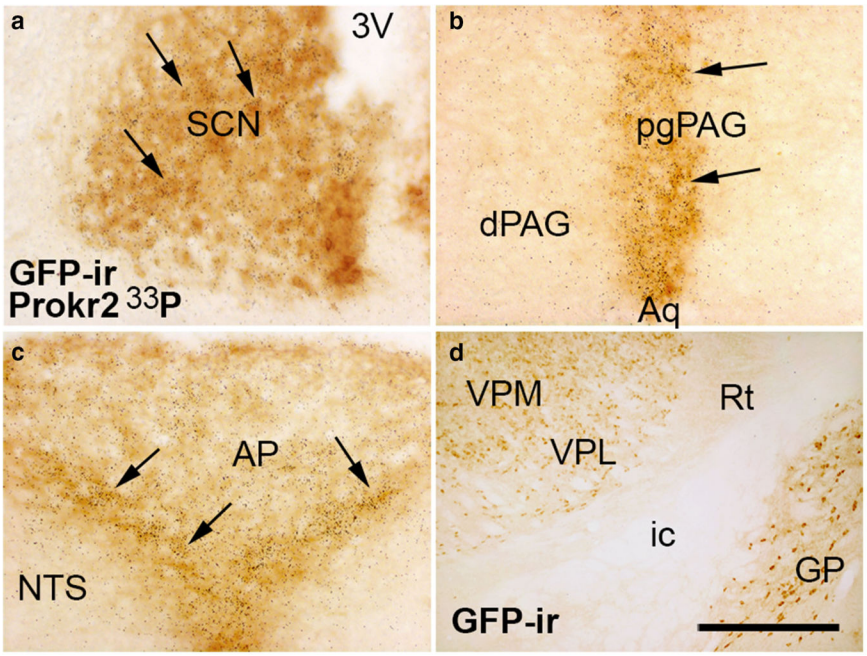

Fig. 4.

Coexpression of Prokr2 mRNA and Prokr2-Cre GFP in the female brain. **a**–**c** Bright field images showing colocalization of Prokr2 mRNA (hybridization signal visualized as dark grains) and Prokr2-Cre GFP immunoreactivity (GFP-ir, *arrows*) in the suprachiasmatic nucleus (SCN, **a**), in the pleioglial periaqueductal gray (pgPAG, **b**) and in the nucleus of the solitary tract (NTS, **c**). **d** Bright field images showing GFP immunoreactive cells in the ventral posterolateral (VPL) and ventral posteromedial (VPM) nuclei of the thalamus. *3V* third ventricle, *AP* area postrema, *Aq* aqueduct, *dPAG* dorsal column of the periaqueductal gray, *GP* globus pallidus, *ic* internal capsule, *ox* optic chiasm, *Rt* reticular nucleus of the thalamus. *Scale bar* **a**–**d** 100 μm

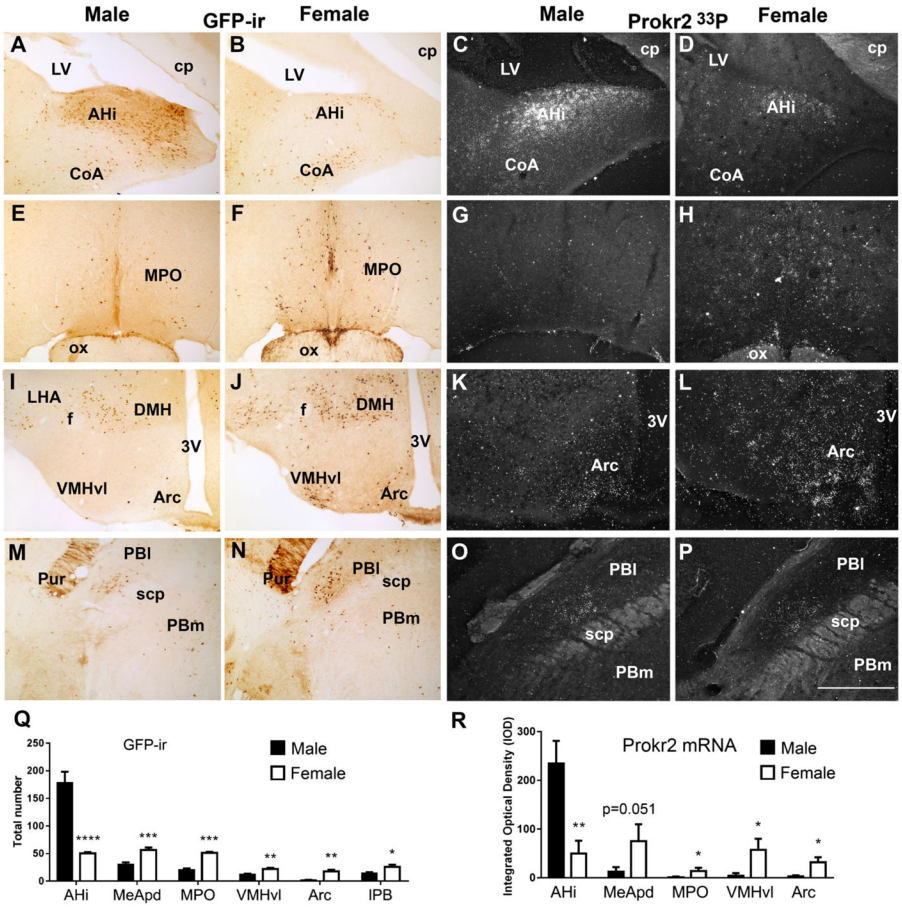

Fig. 5.

Differential expression of Prokr2-Cre GFP and Prokr2 mRNA in adult (P60-P80, G2 generation) male and female brains. **A**, **B**, **D**, **E**, **G**, **H**, **J**, **K** Bright- and dark-field images showing the differential distribution of GFP immunoreactive (GFP-ir) cells and Prokr2 mRNA in male (**A**, **C**, **E**, **G**, **I**, **K**, **M**, **O**) and female (**B**, **D**, **F**, **H**, **J**, **L**, **N**, **P**) brains. **Q** *Bar graphs* showing sexual dimorphism in the number of GFP-ir cells in amigdalo-hippocampal nucleus (AHi, $P = 0.0007$, $q = 0.00036$, t 6.34), posterodorsal subdivision of the medial nucleus of the amygdala (MeApd, $P = 0.003$, $q = 0.00079$, t 4.40), medial preoptic area (MPO, $P = 0.0006$, $q = 0.00068$, t 8.38), in the arcuate nucleus (Arc, $P = 0.0015$, $q = 0.0005$, t 5.03), in the ventrolateral subdivision of the ventromedial nucleus of the hypothalamus (VMHvl, $P = 0.0048$, $q = 0.0009$, t 4.03) and in the lateral parabrachial nucleus (PBl, $P = 0.02$, $q = 0.0043$, t 2.82). **R** *Bar graphs* showing sexual dimorphism of Prokr2 mRNA in AHi ($P = 0.0079$, $q = 0.040$, t 4.91), in MPO ($P = 0.036$, $q = 0.045$, t 2.68), in VMHvl ($P = 0.020$, $q = 0.045$, t 3.13), in Arc ($P = 0.029$, $q = 0.045$, t 2.83) and a strong trend in MeApd ($P = 0.051$, $q = 0.052$, t 2.41). No difference was observed in Prokr2 mRNA in the PBl. *3V* third ventricle, *CoA* cortical nucleus of the amygdala, *cp* cerebral peduncle, *DMH* dorsomedial nucleus of the hypothalamus, *f* fornix, *LHA* lateral hypothalamic area, *LV* lateral ventricle, *ox* optic chiasm, *PBm* medial parabrachial nucleus, *Pur* Purkinje cells, *scp* superior cerebellar peduncle. *P<0.05; **P<0.01; ***P<0.001, ****P<0.0001. *Scale bar* 400 μm

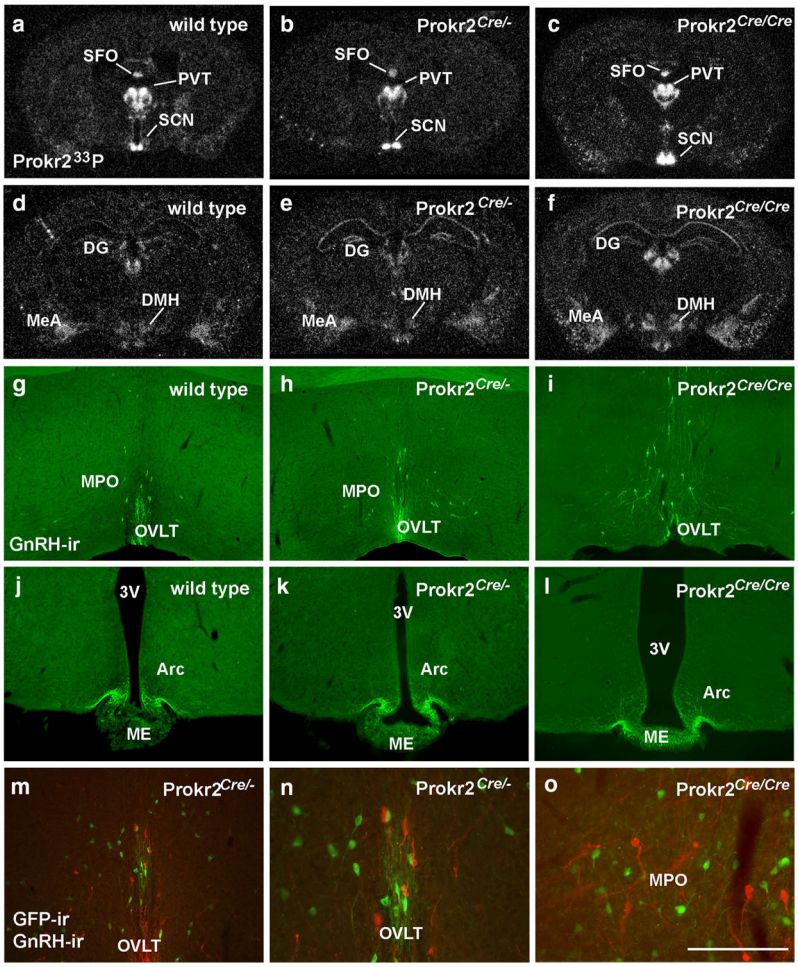

Fig. 6.

Prokr2 mRNA and GnRH neuronal migration are not altered in Prokr2-Cre heterozygous and homozygous mice. **a**–**f** Dark field images showing the distribution of Prokr2 mRNA (hybridization signal observed as silver grains) in the brains of wild type (**a**, **d**), Prokr2-Cre heterozygous (**b**, **e** G3 generation, P60–80 days of age) and Prokr2-Cre homozygous (**c**, **f** G5 generation, P60–70 days of age) females. **g**–**l** Fluorescent images showing the distribution of gonadotropin releasing hormone immunoreactive (GnRH-ir) cell bodies (**g**–**i**) and fibers (**j**–**l**) in wild type (**g**, **j**), Prokr2-Cre heterozygous (**h**, **k**), and ProR2-Cre homozygous (**i**, **l**) female mice. No differences were observed in the distribution of Prokr2 mRNA and GnRH neurons. **m**–**o** Fluorescent images showing distribution of GnRH-ir (*red*) and GFP-ir (*green*) cells in the Prokr2-Cre heterozygous (**m**, **n**) and homozygous (**o**) female mice. Note lack of colocalization and close proximity between these two groups of cells. *3V* third ventricle, *ac* anterior commissure, *Arc* arcuate nucleus, *DG* dentate gyrus, *DMH* dorsomedial nucleus of the hypothalamus, *ME* median eminence, *MeA* medial nucleus of the amygdala, *MPO* medial preoptic area, *OVLT* vascular organ of the lamina terminalis, *PVT* paraventricular nucleus of the thalamus, *SCN* suprachiasmatic nucleus, *SFO* subfornical area. *Scale bar* **a**–**f** 2 mm, **g**–**m** 400 μm, **n**, **o** 200 μm

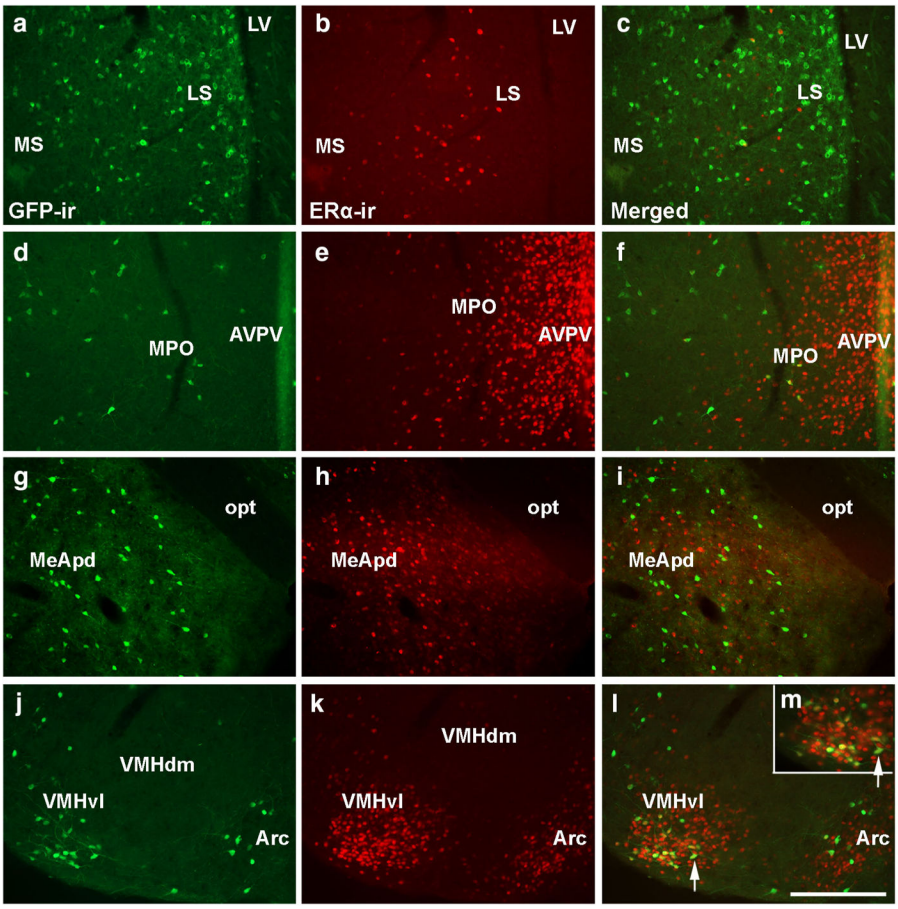

Fig. 7.

Prokr2-Cre GFP and ERα are coexpressed in the ventrolateral subdivision of the ventromedial nucleus of the hypothalamus (VMHvl) in females. **a**–**m** Fluorescent images showing the distribution of GFP immunoreactivity (GFP-ir, **a**, **d**, **g**, **j**) and ERα-immunoreactivity (ERα-ir, **b**, **e**, **h**, **k**) in the lateral septum (LS, **a**–**c**), the medial preoptic area (MPO, **d**–**f**), the posterodorsal subdivision of the medial nucleus of the amygdala (MeApd, **g**–**i**), the arcuate nucleus (Arc, **j**–**l**), and the ventrolateral subdivision of the ventromedial nucleus of the hypothalamus (VMHvl, **j**–**m**) of a female PorkR2-Cre heterozygous mice (P60–80, G5 generation). Consistent colocalization was only observed in the VMHvl. **m** is a higher magnification of **l** (*arrow* indicates the same cell). *AVPV* anteroventral periventricular nucleus, *LV* lateral ventricle, *MS* medial septum, *opt* optic tract, *VMHdm* dorsomedial subdivision of the VMH. *Scale bar* **a**–**l** 200 μm, **m** 100 μm

Table 1

List of primers used for genotyping of the mouse models

Mice	Forward	Size (bp)
Cre-upstream	F 5′ TTCCCTGGTCCCTATGTCAG 3′	1112
	R 5′ GTCCCTGAACATGTCCATCA 3′	
Cre-downstream	F 5′ GTCCATCCCTGAAATCATGC 3′	990
	R 5′ CTCATTGCCACTGGAAACCT 3′	
Cre (founders)	F 5′ GAAATGGTTCCCTGCTGAAC 3′	600
	R 5′ TCTCTGCCCAGAGTCATCCT 3′	
Prokr2-Cre (progeny)	F 5′ TCCCCACGGTAGTTGTGAAG 3′	Cre: 353
	R 5′ ATTGGTTGGTGTGGTTTGCAG 3′	Wt: 499
	mt 5′ CAGCAGGTTGGAGACTTTCCT 3′	
Genomic *iCre* (qPCR)	F 5′ CCACATTGGCAGGACCAAGA 3′	163
	R 5′ GGCAGCCACACCATTCTTTC 3′	
Genomic *Il2* (qPCR)	F 5′ CTAGGCCACAGAATTGAAAGATCT 3′	324
	R 5′ GTAGGTGGAAATTCTAGCATCATCC 3′	
R26-tdTom[a]	F 5′ CTGTTCCTGTACGGCATGG 3′	197
	R 5′ GGCATTAAAGCAGCGTATCC 3′	
R26-GFP[a]	F 5′ AAGTTCATCTGCACCACCG 3′	176
	R 5′ TCCTTGAAGAAGATGGTGCG 3′	

[a]Mouse lines are commercially available at JAX® mice

Table 2

Distribution of Prokr2-Cre GFP immunoreactive neurons and Prokr2 mRNA in adult male and female mice

Brain areas and nuclei	Male		Female	
	Prokr2-Cre GFP-ir	Prokr2 mRNA	Prokr2-Cre GFP-ir	Prokr2 mRNA
Cerebral cortex				
Anterior olfactory	+	+	++	+
Lateral olfactory tract	+	+	++	+
Endopiriform	+	+/−	+	+
Subventricular zone of lateral ventricle	+	++	+	++
Piriform	+	+	+	+
Prelimbic/infralimbic	++	+/−	+++	+
Cingulate	+/−	+	+	+
Retrosplenial	+	+	++	+
Perirhinal	+++	+	+++	++
Entorhinal	+	+/−	+	+
Insular	++	+	++	+
Septum				
Lateral septum, dorsal	+++	+++	+++	+++
Lateral septum, intermediate	++	++	++	++
Lateral septum, ventral	+	+	++	+
Medial septum	+/−	+/−	+	+
Hippocampus				
CA1 and CA3	+	+	+/−	+
Dentate gyrus	+	+/−	++	+
Presubiculum/subiculum	+	+	+	+
Basal ganglia				
Caudado/putamen	+/−	−	+	−
Accumbens	+	+/−	++	+/−
Ventral pallidum	+	+/−	++	+/−
Globus pallidus, lateral ventral	++	++	++	++
Amygdala, bed nucleus of stria terminalis				
Anterior cortical amygdala	+	+	+	+
Lateral amygdala	++	++	++	+
Basomedial amygdala	++	+	++	++
Medial amygdala, posterodorsal	+	+	+++	++
Amygdalohippocampal area	++++	++++	++	++
Amygdalopiriform transition area	+	+	+	+
Bed nucleus of stria terminalis, medial	+/−	+/−	+	+
Thalamus and epithalamus				
Anterodorsal	+	+	+	+
Paraventricular	+++	+++	+++	+++
Paracentral	++	++	++	++

Brain areas and nuclei	Male		Female	
	Prokr2-Cre GFP-ir	Prokr2 mRNA	Prokr2-Cre GFP-ir	Prokr2 mRNA
Central medial	++	++	++	++
Interoanterodorsal	+	+	+	+
Xifoid	++	+	+++	++
Reuniens	+	+/−	++	+
Lateral dorsal	+++	+/−	+++	+
Lateral posterior	++	+/−	++	+
Lateral habenula	+++	++	+++	++
Medial habenula	++	++	++	++
Ventral lateral	+++	−	+++	−
Ventral posteromedial	+++	−	+++	−
Ventral posterolateral	+++	−	+++	−
Hypothalamus				
Median preoptic	+	+/−	+	+
Medial preoptic area	+	+/−	+++	+
Lateral preoptic area	+	+/−	+	+/−
Ventrolateral preoptic	+	−	+	−
Lateral preoptic area	+	−	++	−
Suprachiasmatic	++++	++++	++++	++++
Paraventricular, parvicellular	+++	+++	+++	+++
Lateral hypothalamic area	++	+	++	+
Perifornical area	+++	++	++	++
Arcuate	+	+	++	++
Ventromedial, ventrolateral	−	−	+	+
Dorsomedial	+++	++	+++	++
Dorsal premammillary	+++	+++	+++	+++
Posterior hypothalamus	++	++	++	++
Lateral mammillary	+++	+++	+++	+++
Medial mammillary, medial	++	+++	++	+++
Medial mammillary, lateral	+++	++	+++	++
Midbrain				
Precomissural	+	+	+	+
Superior colliculus	+	+	++	+
Edinger–Westphal	+	+/−	+	+/−
Periaqueductal gray, dorsal	++	+	+++	+
Periaqueductal gray, ventrolateral	++	+	+++	+
Pleioglial periaqueductal gray	++++	++++	++++	++++
Dorsal raphe	++	++	++	++
Hindbrain				
Dorsal cochlear	+	+/−	+	+/−
Parabrachial, medial	+	−	+	−
Parabrachial, lateral	+	+	++	+

Brain areas and nuclei	Male		Female	
	Prokr2-Cre GFP-ir	Prokr2 mRNA	Prokr2-Cre GFP-ir	Prokr2 mRNA
Lateral reticular	+	+/−	+	+/−
Nucleus of the solitary tract, anterior	++	+/−	++	+/−
Dorsal motor (10)	+/−	−	+/−	−
Hypoglossal (12)	+	−	+	−
Cerebellum, Purkinje cells	+	−	+	−
Circuventricular organs				
Subfornical organ	+++	+++	+++	+++
Median eminence	+/−	−	+/−	−
Subcomissural	+++	+++	+++	+++
Area postrema	++++	++++	++++	++++

Subjective analysis comparing number of GFP + cells in Prokr2$^{Cre/+}$ mice (n = 4–5/sex) and hybridization signal in wild type mice (n = 3/sex).

+/−, very low; +, low; ++, moderate; +++, high; ++++, very high